Journal of Structural Geology, Vol. 14, No. 8/9, pp. 905 to 913, 1992
Printed in Great Britain

0191-8141/92 $05.00 + 0.00

The evolution of seismicity at Parkfield: observation, experiment and a fracture-mechanical interpretation

JEREMY HENDERSON and IAN MAIN

Department of Geology and Geophysics, University of Edinburgh, Edinburgh EH9 3JZ, U.K.

and

PHILIP MEREDITH and PETER SAMMONDS

Department of Geological Sciences, University College London, Gower Street, London WC1E 6BT, U.K.

(*Received* 6 *September* 1991; *accepted in revised form* 2 *April* 1992)

Abstract—We compare observations of local seismicity sequences with acoustic emissions during rock fracture, and find similarities in the distribution of event magnitudes which lead us to consider a model of seismicity which is characterized by fracture-growth laws derived from the field of fracture-mechanics and which include both negative and positive feedback processes. We find that the model predicts the observed negative correlation between the seismic b-value and the fractal dimension of the earthquake epicentres. The simple short-range interactions described in the model give rise to a system with a long-range order, similar to current models of critical processes.

INTRODUCTION

ARGUABLY the highest priority in the study of seismology is to provide some means of predicting the occurrence of potentially damaging earthquakes. This question has been studied since well before the current era of instrumental seismology, but rather little practical progress has been made. Following the recent upsurge in interest in the dynamics of non-linear systems, it has been recognized that earthquakes may in fact be an example of a 'chaotic' system and therefore inherently unpredictable. If this is the case, then it may not be immediately fruitful to attempt to study the occurrence of individual earthquakes, and it may instead be of more value to study the phenomenon of 'seismicity', or the statistical characteristics of an ensemble of earthquakes.

It has been recognized for some time that the parameters which describe seismicity in a region show a spatial and temporal evolution which may be associated with the process of the generation of earthquakes. For example, one of the most common means of describing the pattern of seismicity in a given area is the value b in the Gutenberg–Richter relation:

$$\log N = a - bm, \tag{1}$$

where N is the number of earthquakes of magnitude greater than m. Smith (1981) has shown that the value of b in New Zealand has shown a systematic increase in the period preceding large earthquakes.

The recognition that many natural objects or systems are not well described by the familiar figures of geometry, but are better described in terms of fractals (Mandelbrot 1975) suggests that seismicity might also be described in these terms. It might be noted, first of all, from the power-law nature of the Gutenberg–Richter relation that the b-value is itself related to the fractal dimension of earthquake magnitudes (Turcotte 1986), which may be likened to the familiar example of the fractal dimension of sizes of islands in an ocean (Mandelbrot 1975). The fractal geometries of various aspects of fault systems have been investigated, notably the fractal dimension corresponding to the roughness of the trace of the San Andreas fault at the surface estimated by Aviles *et al.* (1986) and Okubo & Aki (1986). We use this evidence of the fractal nature of seismicity as a justification for analysing our data and the results of our numerical simulations in terms of fractal dimensions.

The statistics of acoustic emissions measured in rock samples studied under compression in the laboratory show changes in event rate and b-value similar to those of sequences of naturally occurring earthquakes (Main *et al.* 1990) and so it appears reasonable to conclude that there is an underlying similarity in the physics of the processes that are occurring in the Earth's crust and in laboratory samples, despite the large differences in scale of the processes. We suggest that this similarity between the characteristics of acoustic emissions in the laboratory, which are clearly related to fracture, and the characteristics of sequences of seismic events suggests that it is valid to consider the latter phenomena in which fracture plays an important role. This approach differs from that of Mogi (1962) and Scholz (1968) who linked b-values to (respectively) rock heterogeneity and applied stress. The pre-existence of faults in an area does not necessarily imply that frictional sliding is the sole seismogenic process. This apparent conundrum might be explained by the hypothesis that faults act as conduits for circulating fluids from which cementing materials are

precipitated, particulary in zones with a long repeat time.

Many attempts have been made to produce models of the seismic process which account for the observed magnitude statistics of earthquakes. Huang & Turcotte (1988) considered the effect of applying a stress to a two-dimensional system whose elements had an *a priori* fractal distribution of strengths. Bak & Tang (1989) and Sornette & Sornette (1989) have used the concept of self-organized criticality to develop models which predict a power-law distribution of earthquake energies. However, these models do not explicity model the processes believed to operate during the fracture of rocks.

It is the purpose of this paper to present an analysis of an ensemble of naturally occurring earthquakes which shows a clear example of evolution of the values of the parameters describing this seismicity and their interrelation. We present some results from laboratory experiments which show a similar evolution in event magnitude statistics, and provide a simple model of the failure process based on fracture mechanics. Our numerical modelling differs from that of von Seggern (1980), who modelled the effect on earthquake statistics of a transition from static to dynamic frictional stresses, in that we base our model on studies of rock fracture, which suggest the presence of both positive and negative feedback mechanisms. Cox & Paterson (1990) consider a small two-dimensional network which fractures under the imposition of an external stress, but their model focuses on the explicit calculation of the full perturbed stress field, rather than using an approach based upon stress intensities calculated simply from mean remote stresses and local crack lengths. Yamashita & Knopoff (1989) also consider a model based upon fracture-mechanics, but do not include a negative feedback process.

EVOLUTION OF SEISMICITY AT PARKFIELD, CALIFORNIA

The data used in this analysis were recorded in the Parkfield area of California, between 1970 and 1990. This dataset includes data relating to the nearby major event at Coalinga in 1983, as well as to large events in the Middle Mountain area in 1975. The data relate to a segment of the San Andreas fault about 60 km long, between a fault segment to the north-west which is essentially aseismic, and a segment to the south-east which seems to fail only by catastrophic earthquakes. In order to examine the evolution of earthquake magnitudes over a period of time, it is essential to be certain that the magnitude scale is consistent over the length of the period studied. In the present case, the catalogue has been analysed by Wyss *et al.* (1990) and Wyss (in press), and corrections made to provide magnitude information that is belived to be internally consistent.

The *b*-value was calculated by the maximum-likelihood method (Aki 1985):

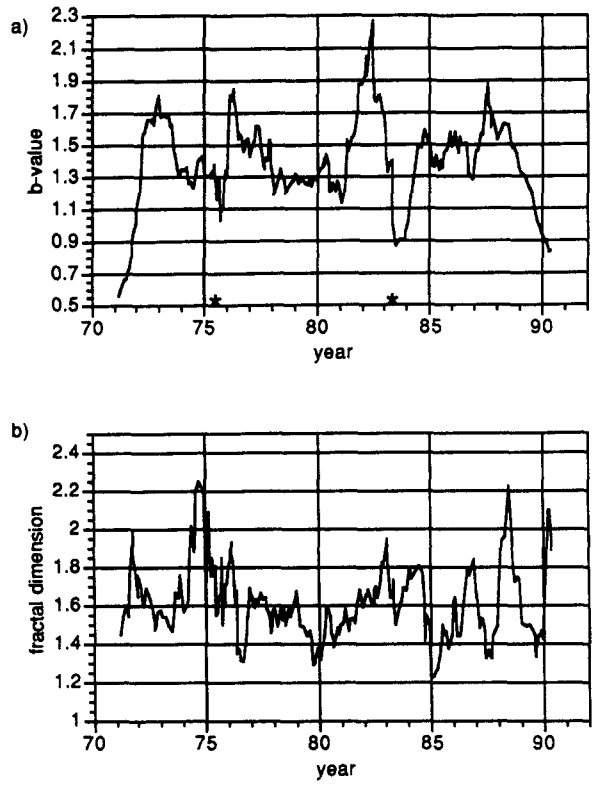

Fig. 1. Graph showing (a) *b*-values and (b) correlation dimensions estimated for the Parkfield area. The time co-ordinate is the date of the last earthquake in the analysis window. The same 100 event analysis windows are used in Fig. 2

$$b = \frac{\log_{10} e}{\bar{m} - m_0}, \tag{2}$$

where $\bar{m}$ is the average magnitude and m_0 is the threshold magnitude for complete reporting of earthquake magnitudes. In this case the threshold magnitude used was 1.3. The *b*-value was calculated for windows of 100 consecutive events and the window was advanced by 10 events between each calculation. The calculated *b*-values are shown in Fig. 1(a). The asterisks on the time axis indicate the time of large earthquakes: the Middle Mountain events of 1975 (magnitude 4.5) and a major event which occurred on 2 May 1983 (the magnitude 6.7 Coalinga earthquake). Note that the *b*-value shows an increase before the event followed by a decrease in the post-event phase over a time-scale of around 1 year.

Figure 2(a) shows the average magnitudes and Fig 2(b) the rates of occurrence of events above the threshold magnitude. Note that this quantity also shows a systematic relationship with the occurrence of major events. For example, the event rates are higher during the period preceding the Coalinga event.

The fractal dimension of the earthquake epicentres was calculated for the same event windows. It should be emphasized at this point that this fractal dimension is fundamentally different from other fractal dimensions, such as that of earthquake sizes (related to the *b*-value), and one need not, *a priori*, expect any correlation between the two. One might, in principle, calculate a fractal dimension for the earthquake hypocentres, but the errors in estimating earthquake depths suggest than

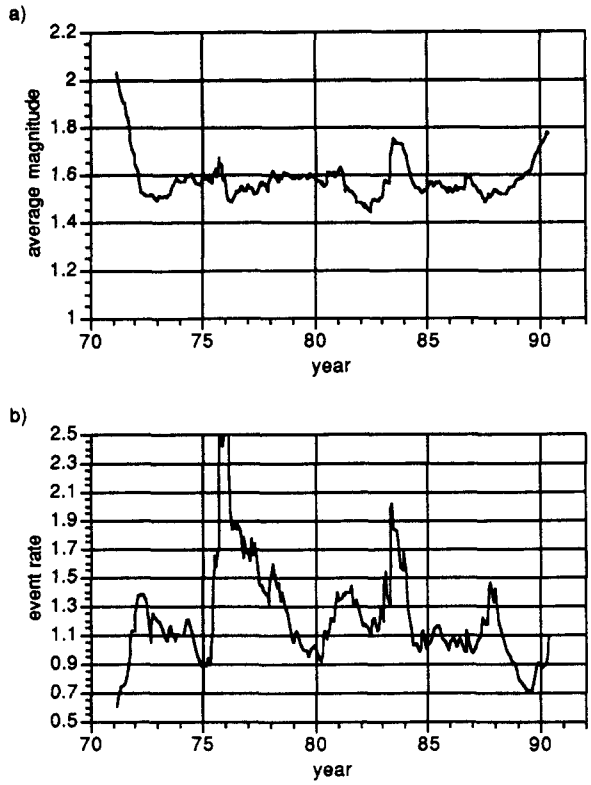

Fig. 2. Graph showing (a) average magnitudes and (b) event-rates estimated for the Parkfield area. The abscissa values are the numbers of events per 100th of a year.

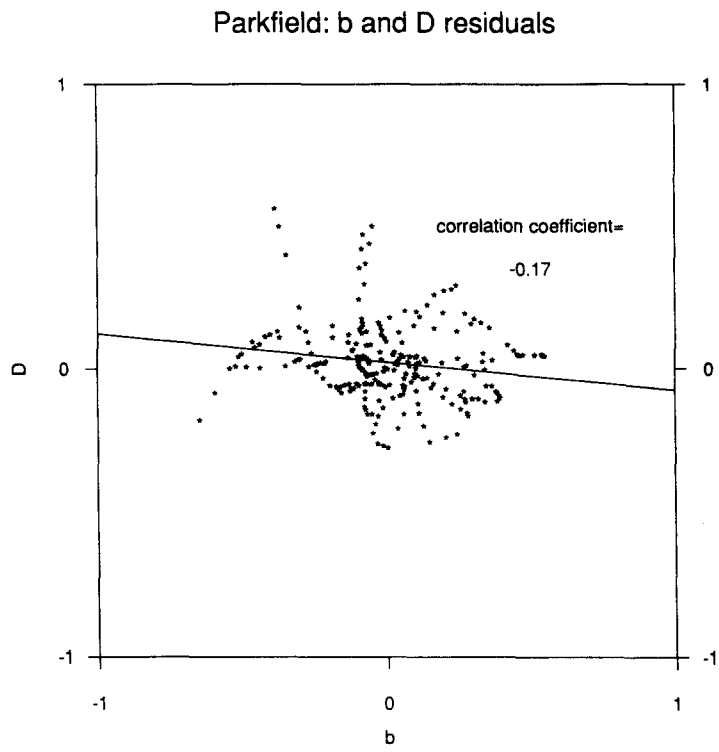

Fig. 3. Graph showing correlation of b-value residuals and correlation dimension residuals for the Parkfield area, and the least-squares best-fitting line.

any attempt to find such a quantity would be prone to much greater errors than those involved in using the epicentres. The fractal dimension was estimated as the correlation dimension, which has been shown to be a good estimate of the fractal dimension (Grassberger & Procaccia 1983). The correlation dimension, D_C, is found from:

$$D_C = \lim_{r \to 0} \frac{\log C(r)}{\log r}, \tag{3}$$

where r is the radius of a circle on the Earth's surface and $C(r)$ is the correlation integral:

$$C(r) = \lim_{N \to \infty} \frac{1}{N^2} \sum_{i,j=1}^{N} H(r - |\mathbf{x}_i - \mathbf{x}_j|), \tag{4}$$

where N is the number of points in the analysis window, $\mathbf{x}$ are the co-ordinates of the epicentres and H is the Heaviside step function: $H(x) = 0$ for $x < 0$; $H(x) = 1$ for $x > 0$.

The calculated correlation dimensions are shown in Fig. 1(b). Examination of Fig. 1 suggests a relationship, there being an apparent negative correlation between b and D_C. This relationship is examined further by subtracting a low frequency trend from each of the b and D_C curves, and plotting these residuals against each other, along with a least-squares best-fitting straight line (Fig. 3). A correlation coefficient of -0.17 was calculated for these data, indicating a weak negative correlation. In spite of the care taken to ensure that the earthquake magnitude information was consistent throughout the catalogue, there may remain doubts that the b-value anomalies associated with large earthquakes are simply artefacts caused by, for example, saturation of recording networks. However, we can conceive of no reason why these doubts should apply to the epicentre information from which the correlation dimensions are calculated. We conclude, therefore, that this analysis represents a valid example of the negative correlation between b-value and epicentre correlation dimension. Our results may therefore be compared with that of Hirata (1989), who found a weak negative correlation between b-value and correlation dimension for earthquakes in Japan.

LABORATORY EXPERIMENTS ON ROCK FRACTURE: b-VALUES

Triaxial deformation tests have been performed in the laboratory on intact samples of Darley Dale sandstone, a hard feldspathic sandstone (Sammonds *et al.* 1989). A confining pressure of 50 MPa was applied, and an additional compressive load applied via a servo-controlled actuator. The strain rate was maintained at 10^{-5} s^{-1}, and a constant pore fluid volume was preserved ('undrained' test). During the experiment, acoustic emissions were detected by piezo-electric sensors, and the peak amplitudes of single events measured. The seismic b-value was calculated for emissions during periods of 30 s. The b-value is calculated using the Aki maximum-likelihood formula by identifying the decibel value of the acoustic emission with an earthquake magnitude.

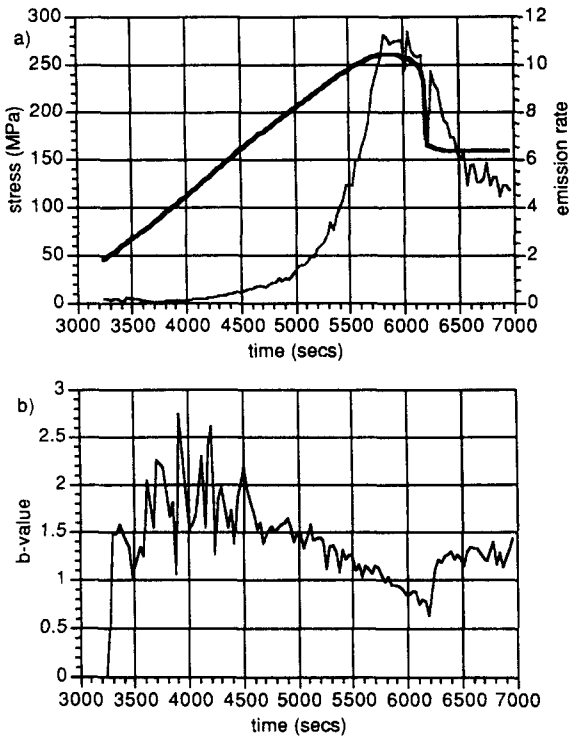

Fig. 4. (a) Measurements of stress (heavy line) and event-rate (thousands of emissions per logging interval) and (b) b-values during deformation of Darley Dale sandstone in the laboratory.

An example of a typical set of results is shown in Fig. 4. At low stresses, corresponding to times less than 3000 s, the event rate is low, and meaningful b-values are not calculated. The failure of the sample is marked by an abrupt drop in stress at 6200 s. The figure shows a maximum in the b-value at around 4000 s, preceding a minimum coincident with failure of the specimen by fracture. The pre-failure phase is also characterized by high event rates. We interpret this similarity between the behaviours of event rates and b-values as suggesting that similar processes occur in the Earth's crust during the generation of earthquakes as in the laboratory during fracture, and on this basis we seek to explain these phenomena in terms of a fracture-mechanical model.

FRACTURE-MECHANICAL MODEL

Description of the model and its basis

We consider a 'fault' to be an isolated one-dimensional feature composed of a series of differing fracture toughnesses. The whole fault is subject to a uniform remote stress, but locally the stress may be modified by the existence of cracks. By 'crack' we mean an element, or series of elements, whose fracture toughness is exceeded by the local stress. We specifically examine two effects which occur as the remote stress is increased: the effect of introducing an isolated crack into the fault, and the effect on crack evolution of the interaction of nearby cracks. Our model is one-dimensional in the sense that the fault is represented by a one-dimensional array of elements, but the remotely applied stress might be imagined to be applied in some direction in the two-dimensional plane containing the fault, for example, a tensile stress applied perpendicular to the fault. This section describes the processes modelled, and introduces the manner in which they are incorporated into our one-dimensional model.

When a crack is introduced into a material under stress, the stress field in the vicinity of the crack is modified. The manner of this modification is described by the stress intensity factor, K. In a simple model of extensional fracture (Griffith 1924) an initial flaw in the sample would develop into a crack which grows rapidly as the stress in the vicinity of the crack tip is amplified by the presence of the crack itself. Crack growth continues as long as the local stress intensity factor exceeds the critical level, or fracture toughness, K_C. Observation of fracture development during compressional loading, however, suggests that this model is not applicable to this case, and that prior to failure the sample suffers widespread damage (Peng & Johnson 1975, Wong 1982, Cox & Scholz 1988). The nature of this damage depends upon the experimental conditions such as the speed and configuration of loading and the presence of a chemically active pore fluid (Main *et al.* 1990). Under compression, cracks are observed to grow parallel to the principal axis of compression (Tapponnier & Brace 1976). In the early stages of damage, crack growth is not continuous, and appears to stop when the stress has been locally relieved. This relief of stress has been analysed for the case of growing wing cracks by Ashby & Hallam (1986) who show that initially such tensile cracks grow stably under a compressive deviatoric stress field, and instability only develops when the mean crack length approaches the mean crack separation. The general features of our model are illustrated in the cartoon in Fig. 5.

Costin (1983, 1987) has described the same phenomenon in terms of a 'domain' surrounding a growing crack. Initially the crack is deemed to relieve the stress intensity within the 'domain' and growth is inhibited as the crack semi-length approaches the radius of the 'domain'. We follow Costin (1987) by assuming that the reduction of stress intensity factor, K, at the crack tip is described by:

$$K \propto S_r \left(\frac{d-a}{d}\right)(\pi a)^{1/2}, \tag{5}$$

where S_r is the remote stress, d is the radius of the 'domain' and a is the crack half-length. This equation is unlikely to be correct in detail, but it conserves the essential physical idea that under compression, growth of individual cracks occurs in a stable mode, and is unlikely to be the cause of dynamic failure. The stability of this quasi-static state of damage is due to the negative feedback between the increase in crack length and the stress intensity, represented by the term $(d-a)/d$ in equation (5).

We adopt a similar approach to the question of crack

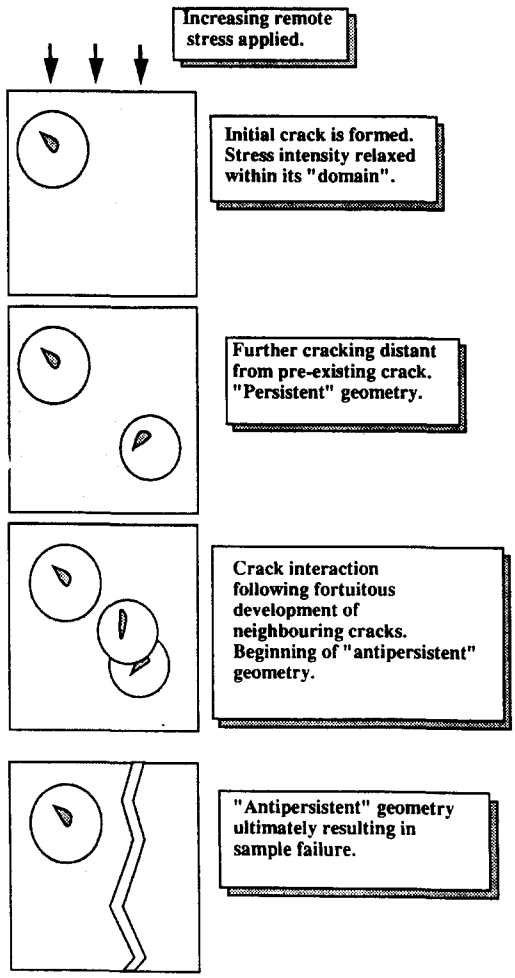

Fig. 5. Cartoon to illustrate the processes believed to be occurring during the fracture of rocks.

interaction, which is now known to be the dominant process leading to rock failure in compression (Wong 1982), and which has been studied in detail by, for example, Nemat-Nasser & Horii (1982), Horii & Nemat-Nasser (1985) and Ashby & Hallam (1986). The complexity of this problem has meant that analytical solutions are only available for special geometries of interacting cracks, for example, an infinite series of identical cracks (Irwin 1957), but comparisons of the solutions obtained using different approaches (Rudnicki & Kanamori 1981; Costin 1987), suggest that useful results can be obtained using a simple expression to calculate the stress concentration in the region between nearby cracks. The main feature of all of these models is that the stress intensity at the tip of a crack is increased by the presence of a neighbour, and the stress in the intervening region is also increased. This corresponds to a positive feedback in the crack's growth process, eventually leading to a runaway instability. Following Rudnicki & Kanamori (1981) we use the equation:

$$K \propto S_r (c \tan(\pi a/2c))^{1/2}, \qquad (6)$$

where c is the centre-to-centre distance between adjacent cracks.

Equations (5) and (6) show the effect of the 'domain of stress intensity relaxation' and 'crack interaction' for the elements which are at the tips of growing cracks. The way in which the stress intensity factor changes as we move away from the crack tip is not known. We assume in this work that the 'stress intensity relaxation' effect declines exponentially away from the crack tip, and that the 'interaction effect' declines according to a tangent law. In principle, therefore, the stress intensity factor in every fault element is affected by the existence of even a modest number of cracks. In practice, however, this effect is negligible except for the fault elements in the close vicinity of a crack.

Figure 6 illustrates the algorithm with which these ideas are applied to our model. Each fault element is assigned a critical stress intensity, K_C, or 'fracture toughness'. The fracture toughnesses are initialized as steps in a 'random walk', i.e. the fracture toughness of each element is greater than that of its neighbour by the length of a 'step'. The step lengths are selected randomly from a zero-mean Gaussian distribution and shifted so as to make all element fracture toughnesses initially positive. The random walk is chosen as a means of initializing the model because it is a good approximation to many processes found in nature (Mandelbrot 1977). It is supposed that each of the fault elements will contain small flaws which will propagate (resulting in failure of the fault element) when the critical stress intensity factor for that element, K_C, is exceeded by the local stress intensity factor. The local strength, then, is a function of the fracture toughness and of the lengths of nearby cracks. For simplicity, we imagine that the remote stress will give rise to a general stress intensity factor which is uniform over the fault in the absence of failed elements. The local stress intensity factor, however, is a function of the remotely applied stress and the presence of cracks (fault segments of one or more adjacent failed fault elements). The remote stress is incrementally increased by a constant amount at each step, and the effect of this increase and the resulting changes on local stress, and hence the distribution of cracks, is examined at each step using equations (5) and (6). The iteration is considered to be complete when a stable configuration, with no unfailed fault elements having lower K_C than the local stress intensity factor, has been attained.

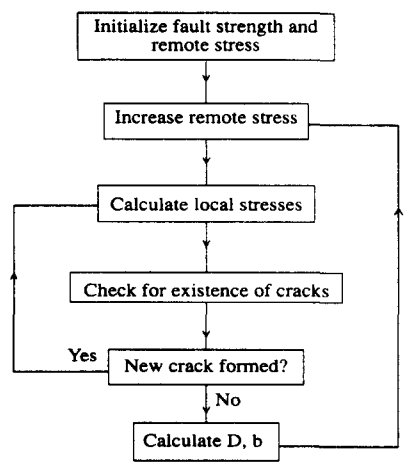

Fig. 6. Flowchart to illustrate the algorithm used to model crack growth in the one-dimensional model described in this paper.

Before incrementing the stress, the crack sizes and distributions are analysed by calculation of a fractal dimension, and by calculating a b-value. Whereas the b-value for earthquakes is commonly estimated using equation (2), in the case of a model such as this it is less clear how to identify 'crack length' with earthquake magnitude. We calculate b-values assuming that magnitude scales logarithmically with crack length, with m_0, the threshold magnitude for complete reporting of earthquake magnitudes, taken as zero, corresponding to the fracture of a single element. This is consistent both with a simple dislocation model of the seismic source (Kanamori & Anderson 1975) and with the power-law distribution of fault associated with a fractal distribution.

The fractal dimension, D is measured using a 'box-counting' method, as described, for example, by Feder (1989). This is a standard method for the computation of a fractal dimension and was chosen for computational convenience. The numbers of 'boxes' needed to cover the cracks are plotted against the sizes of boxes used, on log–log axes, the fractal dimension being the negative slope of a straight line passing through the points plotted. An example of this measurement is shown in Fig. 7. The extent to which this estimate of a fractal dimension is valid may be judged from the straightness of the line on Fig. 7. This indicates fractal behaviour over the range of scales shown.

The Hurst number (H) is calculated as:

$$H = n - D, \tag{7}$$

where n is the Euclidean dimension of the system. In our case, $n = 1$ and hence $0 < D < 1$, while $1 > H > 0$. $H > 0.5$ suggests a predictability or persistence of the system (Feder 1989), while $H < 0.5$ suggests a clustering or anti-persistence.

Observations

Experiments were conducted using faults of different lengths, and all showed similar behaviour. A large 'fault' array is desirable for collecting adequate statistics of crack lengths, but obviously requires greater computational resources. In practice a fault length of 1024 elements was used to investigate a large region of parameter space, and individual situations investigated using a larger array. A cartoon of the general effects observed is shown in Fig. 8. As the remote stress level is increased, the fracture toughness of a part of the fault (Fig. 8a) is exceeded. If this part is isolated, the fault may be inhibited from growing by local relaxation of the stress intensity according to equation (5), even though the remote stress level is increased (Fig. 8b). However, if nearby parts of the fault fail, the stress intensity in the intervening segment may be sufficiently intensified (equation 6) to cause the failure of elements whose fracture toughness is greater than the general stress intensity level. The former corresponds to negative feedback in the local stress intensity with respect to crack growth, and the latter to positive feedback and incipient instability.

In the initial stages of the experiment, failure tends to occur on isolated fault segments, and failure adjacent to these cracks is inhibited. This leads to patches showing well-ordered crack distributions with low fractal dimension, less than 0.5, and high values of b, because of the predominance of small cracks. The Hurst number will

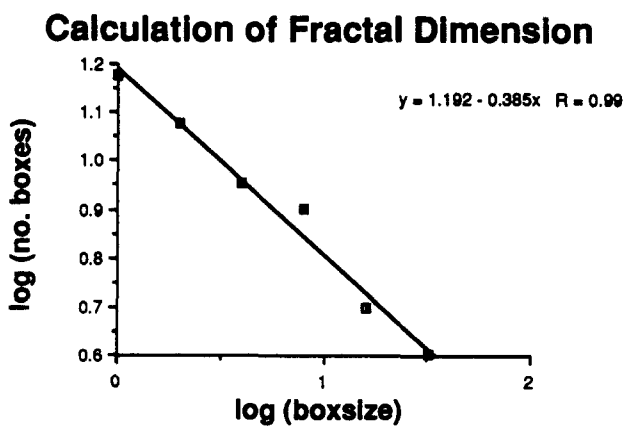

Fig. 7. Example illustrating the calculation of the fractal dimension, D, which is given by the negative gradient of the line fit to the points, which represent the number of 'boxes' of a certain size required to cover the failed elements.

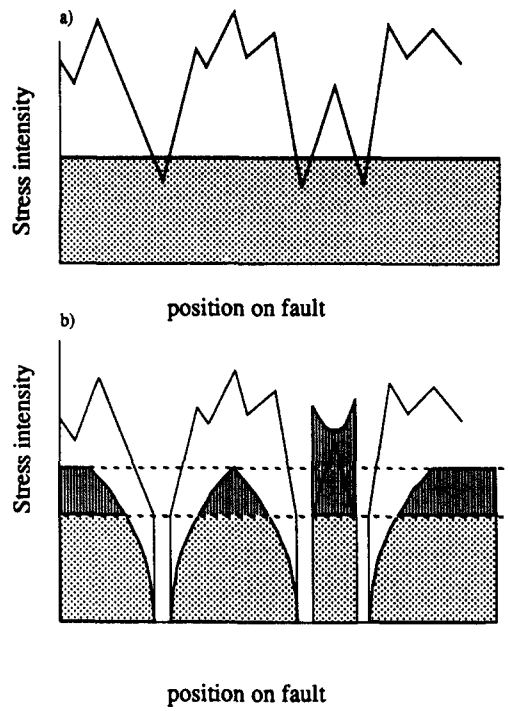

Fig. 8. Cartoon to illustrate the evolution of strengths of fault elements and their influence on local stress intensities. The irregular line represents the strength (K_C) of the fault elements. In the upper figure, three parts of the fault have a lower strength than the general stress intensity level (represented by the dotted area), and form cracks. In the lower figure the general stress intensity level has increased to the level indicated by the heavily shaded area. It can be seen that the crack on the left has relaxed the stress in its neighbourhood, and hence has not grown, despite the higher general stress intensity level. However, the two cracks on the right have interacted to intensify the stress between them, causing failure of a fault segment, even though its strength is greater than the general stress intensity level.

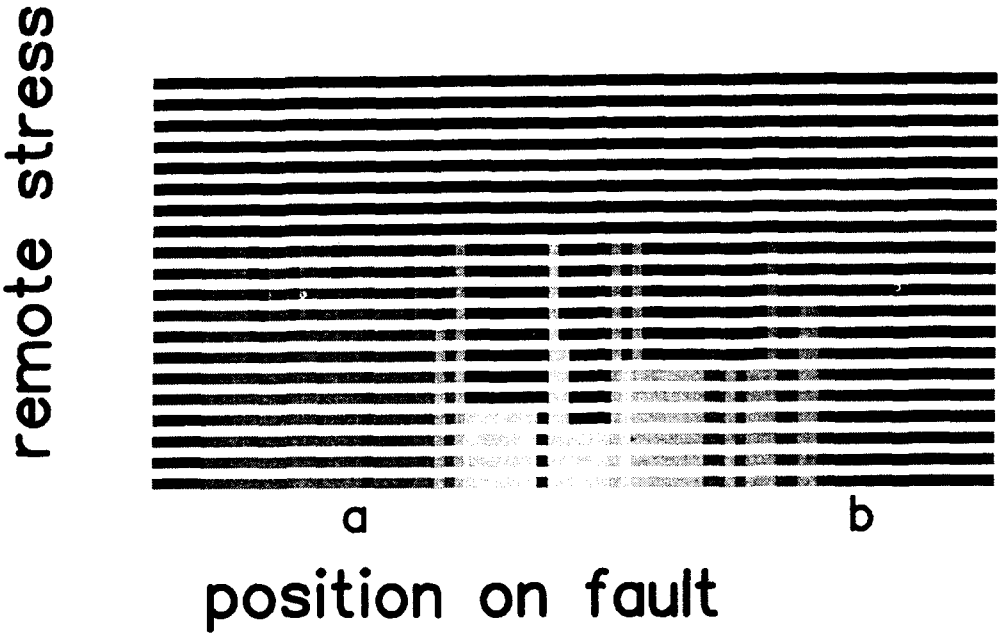

Fig. 9. Diagram showing the 'strength' (fracture toughness) of fault elements of a part of the fault. The strength of elements are coded as weak (light grey) to strong (dark grey). Failed elements are shown as black.

therefore be greater than 0.5, showing that these geometries lie in the 'persistent' regime (Feder 1989). This term, implying a predictability of crack location (they are more evenly spaced than for a random distribution—$H = 0.5$), applies solely to the geometry of the cracks, and not the the physical process taking place, which is, in this case, a sort of negative feedback in the sense described above.

As the experiment proceeds, the likelihood increases that two or more cracks will occur in the same neighbourhood despite the relaxation in stress, and this results in patches in which failure occurs as a result of crack interaction, with a consequent decline in b-value. Eventually the whole fault is consumed by this process and the the b-value declines rapidly during a catastrophic phase. An illustration of the evolution of part of the fault is shown in Fig. 9. Note that the elements indicated as 'a' and 'b' have the same fracture toughness, but element 'a' fails before element 'b' because of the effects of nearby cracks. The evolution of b-value and fractal dimension are shown in Fig. 10(a). This figure may be compared with Fig. 10(b) which shows the evolution of seismicity observed for a model in which nearby cracks had no intensifying influence on the local stress. The model including both negative and positive feedback mechanisms shows a fractal dimension which rises steadily with increasing remote stress, reflecting the manner in which the cracks occupy more and more of the space. During periods dominated by crack coalescence, the b-value is in anti-correlation with the fractal dimension, a situation observed in natural seismicity in Japan (Hirata, 1989). This figure may also be compared with the observations of Smith (1981) and Main *et al.* (1989). In contrast, the model including only negative feedback shows, following an initial anomalous period, a monotonic increase in b-value and fractal dimension.

DISCUSSION

Observations of seismicity suggest a relationship between the distribution of earthquake magnitudes and the distribution of earthquake epicentres. Hirata (1989) has shown that the b-value and fractal dimension of epicentres, measured by a two-point correlation dimension in the Tohoku region of Japan, show a negative correlation, and we find that the same re-

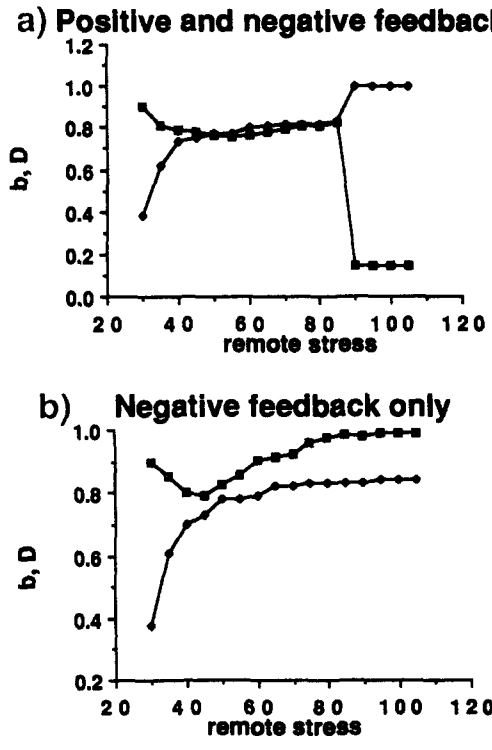

Fig. 10. (a) Graph showing how the b-value (squares) and fractal dimension, D (diamonds), of the fault evolve as the remote stress level is increased. (b) As Fig. 4(a), but for a model in which crack interaction does not influence the stress between cracks.

lationship holds in the case of earthquakes occurring in the Parkfield area. The evolution of b-value has been reproduced during fracture experiments on natural rock samples, suggesting that the processes observed in the laboratory may be occurring on a larger scale during the seismic cycle, and that it is appropriate to seek to explain the features of seismicity in terms of a fracture-mechanical model. These observations imply a large-scale organization, with a power-law distribution of crack sizes and a fractal pattern of earthquake epicentres. An important question is how such a large-scale organization can arise in the absence of long-range interactions.

The model of Huang & Turcotte (1988) produces a power-law distribution of 'earthquake' sizes from a pre-existing fractal distribution of fault fracture toughnesses. It may be true that natural faults have an organized pattern of fracture toughnesses, but it is nevertheless interesting to observe that the simple rules we employ here, which describe only short-range effects can give rise to a realistic sequence of configurations which pervade the whole system. In this respect our model is reminiscent of current models of critical phenomena (e.g. Bak *et al.* 1987, Bruce & Wallace 1989). Because our model does not deal solely with nearest-neighbour interactions, and is not based on integer arithmetic, it would not be correct to refer to it, *sensu stricto*, as a cellular automaton. However, it is informative to compare our model with other models of seismicity which have been presented recently: for example, the family of models based upon the concept of a network of blocks which are connected by springs and which slide under friction on a plane. This frictional model was originally proposed by Burridge & Knopoff (1967). It has been adapted to consideration of a large array of sliding blocks by Carlson & Langer (1989), and this idea has been cast in the form of a cellular automaton model by Rundle & Brown (1991). Such models do not include an explicit negative feedback mechanism, but are governed by a stick–slip frictional law which prevents sliding until a certain threshold has been reached. Positive feedback is provided by the velocity-weaking characteristics of the frictional law employed. It has been hypothesized that these cellular automaton models give rise to a long-range order in a similar way to the manner in which a simple 'sand avalanche' model (e.g. Bak & Tang 1987) gives rise to a self-organized critical system with a power-law distribution of avalanche sizes. Our model produces a similar long-range order, based on simple short-range interactions, but does not resemble a self-organized critical system, because it does not reach a state of dynamic equilibrium. Rather, it leads through a sequence of ordered states to a catastrophic change. In this respect it bears more resemblance to a system undergoing a phase transition.

CONCLUSIONS

We have analysed data from naturally occurring seismic events occurring over a period of around 15 years, and from acoustic emissions generated during laboratory experiments on rock fracturing, and have concluded that the similarity between the evolutions of b-values and event-rates suggests that fracture-mechanical phenomena play an important rôle in determining the evolution of seismicity. On this basis we have constructed a simple model of fracture incorporating the short-range processes believed to be applicable to fault material, and have shown that these processes can give rise to positive and negative feedback scenarios and persistent and anti-persistent geometries of failure. It is well known from the study of universality in physics (Bruce & Wallace 1989) that one of the most important parameters in determining the behaviour of critical systems is the dimension of the space in which this physical system exists. From this observation it is evident that the precise values of, say, fractal dimensions, and their evolution, cannot be derived from our model, since we are simulating a process which occurs in three dimensions by considering a one-dimensional model. Furthermore, it is clear that the precise form of these processes is not accurately described by our algorithm. Nevertheless the results obtained for the global properties of the system show a good agreement with the observations of failure during both natural seismicity and laboratory experiment. Noting that a variety of physical situations (for example, magnetic and chemical phase changes) are recognized to lead to similar global geometries (Bruce & Wallace 1989), our results may be seen as being in accord with the idea that the study of rock failure can be related to that of critical phenomena.

Acknowledgements—The Parkfield catalogue was provided by the United States Geological Survey. The experimental work was funded by NERC grant GR3/6812 and J. Henderson is supported by a NERC Research Studentship. We are grateful to Simon Cox and an anonymous reviewer for their helpful comments on this paper.

REFERENCES

Aki, K. 1965. Maximum likelihood estimate of b in the formula log $N = a - bm$ and its confidence. *Bull. Earthquake Res. Inst. Tokyo Univ.* **43**, 237–239.

Ashby, M. F. & Hallam, D. 1986. The failure of brittle solids containing small cracks under compressive stress states. *Acta metall.* **34**, 497–510.

Atkinson, B. K. 1987. Introduction to fracture mechanics and its geophysical applications. In: *Fracture Mechanics of Rock* (edited by Atkinson, B. K.). Academic Press, London.

Aviles, C. A., Scholz, C. H. & Boatwright, J. 1986. Fractal analysis applied to characteristic segments of the San Andreas fault. *J. geophys. Res.* **92**, 331–334.

Bak, P. & Tang, C. 1989. Earthquakes as self-organized critical phenomena. *J. geophys. Res.* **94**, 15,635–15,637.

Bak, P., Tang, C. & Wiesenfeld, K. 1987. Self organized criticality: an explanation of $1/f$ noise. *Phys. Rev. Lett.* **59**, 381–384.

Brown, S., Rundle, J. B. & Scholz, C. H. 1990. A simplified spring block model of earthquakes. Presented at the Int. Symp. on Earthquake Source Physics and Earthquake Precursors, Tokyo.

Bruce, A. & Wallace, D. 1989. Critical point phenomena: universal physics at large length scales. In: *The New Physics* (edited by Davies, P.). Cambridge University Press, Cambridge.

Burridge, R. & Knopoff, L. 1967. Model and theoretical seismicity. *Bull. seism. Soc. Am.* **57**, 341–347.

Carlson, S. M. & Langer, J. S. 1989. Mechanical model of an earthquake fault. *Phys. Rev.* **A40**, 6470–6484.

Costin, L. S. 1983. A microcrack model for the deformation and failure of brittle rock. *J. geophys. Res.* **88**, 9485–9492.
Costin, L. S. 1987. Deformation and failure. In: *Fracture Mechanics of Rock* (edited by Atkinson, B. K.). Academic Press, London.
Cox, S. J. D. & Paterson, L. 1990. Damage development during rupture of heterogeneous brittle materials: A numerical study. *Spec. Publs geol. Soc. Lond.* **54**, 57–62.
Cox, S. & Scholz, C. H. 1988. Rupture initiation in shear fracture of rocks: an experimental study. *J. geophys. Res.* **93**, 3307–3320.
Feder, J. 1989. Fractals. Plenum Press, New York.
Grassberger, P. & Procaccia, I. 1983. Measuring the strangeness of strange attractors. *Physica* **9D**, 189–208.
Griffith, A. A. 1924. The theory of rupture. In: *Proc. 1st Int. Cong. Appl. Mech.* (edited by Biezeno, C. B. & Burgers, J. M.). Tech. Boekhandel en Drukkerij, Delft, 54–63.
Hirata, T. 1989. A correlation between the *b*-value and the fractal dimension of earthquakes. *J. geophys. Res.* **94**, 7507–7514.
Horii, H. & Nemat-Nasser, S. 1985. Elastic fields of interacting inhomogeneities. *Int. J. Solids Struct.* **7**, 731–745.
Huang, J. & Turcotte, D. 1988. Fractal distributions of stress and variations of *b*-value. *Earth Planet. Sci. Lett.* **91**, 223–230.
Irwin, G. R. 1957. Analysis of stresses and strains near the end of a crack traversing a plate. *J. Appl. Mech.* **24**, 361–364.
Kanamori, H. & Anderson, D. 1975. Theoretical basis of some empirical relations in seismology. *Bull. seism. Soc. Am.* **65**, 1073–1095.
Main, I. G., Meredith, P. G. & Jones, C. 1989. A reinterpretation of the precursory seismic *b*-value anomaly from fracture mechanics. *Geophys. J.* **96**, 131–138.
Main, I. G., Peacock, S. & Meredith, P. G. 1990. Scattering attenuation and the fractal geometry of fracture systems. *Pure & Appl. Geophys.* **133**, 283–304.
Mandelbrot, B. B. 1975. *Les Objets Fractals*. Editions Flammarion, Paris.
Mandelbrot, B. B. 1977. *The Fractal Geometry of Nature*. W. H. Freeman, New York.
Meredith, P. G. & Main, I. G. 1990. Temporal variations in seismicity during quasi-static and dynamic rock failure. *Tectonophysics* **175**, 249–268.
Mogi, K. 1962. Study of elastic shocks caused by the fracture of heterogeneous materials, and their relations to earthquake phenomena. *Bull. Earthquake Res. Inst. Tokyo Univ.* **40**, 125–173.
Nemat-Nasser, S. & Horii, H. 1982. Compression-induced nonplanar crack extension with application to splitting, exfoliation and rockburst. *J. geophys. Res.* **87**, 6805–6821.
Okubo, P. G. & Aki, K. 1986. Fractal geometry in the San Andreas fault system. *J. geophys. Res.* **92**, 345–355.
Peng, S. & Johnson, A. M. 1972. Crack growth and faulting in cylindrical specimens of Chelmsford granite. *Int. J. Rock Mech. & Mining Sci.* **9**, 37–86.
Rudnicki, J. W. & Kanamori, H. 1987. Effect of fault interaction on moment, stress drop and strain energy return. *J. geophys. Res.* **86**, 1785–1793.
Rundle, J. B. & Brown, S. 1991. Origin of rate dependence in frictional sliding. *J. Stat. Phys.* **65**, 403–412.
Sammonds, P. R., Ayling, M. R., Meredith, P. G., Murrell, S. A. F. & Jones, C. 1989. A laboratory investigation of acoustic wave velocity changes during rock failure under triaxial stress. In: *Rock at Great Depths* (edited by Maury, V. & Fourmaintraux, D.). Balkema, Rotterdam, 233–240.
Scholz, C. H. 1968. The frequency-magnitude relation of microfracturing in rock and its relation to earthquakes. *Bull. seism. Soc. Am.* **58**, 399–415.
Smith, W. D. 1981. The *b*-value as an earthquake precursor. *Nature* **289**, 136–139.
Sornette, A. & Sornette, D. 1989. Self organized criticality and earthquakes. *Europhys. Lett.* **9**, 197–202.
Tapponnier, P. & Brace, W. F. 1976. Development of stress-induced microcracks in Westerley granite. *Int. J. Rock Mech. & Mining Sci. Abs.* **24**, 361–364.
Turcotte, D. 1986. Fractals and crustal deformation. *Tectonophysics* **132**, 261.
von Seggern, D. 1980. A random stress model for seismicity statistics and earthquake prediction. *Geophys. Res. Lett.* **7**, 637–640.
Wong, T.-F. 1982. Micromechanics of faulting in Westerley granite. *Int. J. Rock Mech. & Mining Sci. Abs.* **19**, 49–64.
Wyss, M. In press. Changes of mean magnitude of Parkfield seismicity: a part of the precursory process? *Geophys. Res. Lett.*
Wyss, M., Bodin, P. & Habermann, R. E. 1990. Seismic quiescence at Parkfield: an independent indication of an imminent earthquake. *Nature* **345**, 426–428.
Yamashita, T. & Knopoff, L. 1989. A model of foreshock occurrence. *Geophys. J.* **96**, 389–399.